

1 **Sources of Hepatic Glycogen Synthesis in Mice Fed with Glucose or Fructose as the Sole Dietary**
2 **Carbohydrate**

3 Ivana Jarak¹, Cristina Barosa², Fatima O. Martins², Joao C. P. Silva², Cristiano Santos², Getachew
4 Debas Belew², Joao Rito², Ivan Viegas^{1,2}, Jose Teixeira², Paulo Oliveira² and John G. Jones^{2,3*}

5
6 ¹ Centre for Functional Ecology, Department of Life Sciences, University of Coimbra, Portugal

7 ²Center for Neurosciences and Cell Biology, University of Coimbra, Portugal

8 ³APDP-Portuguese Diabetes Association, Lisbon Portugal

9
10 ***Address for Correspondence:**

11 John G. Jones, D.Sc.

12 Center for Neurosciences and Cell Biology

13 UC-Biotech, Biocant Park

14 3060-197, Cantanhede, Portugal

15
16 email: john.griffith.jones@gmail.com

17
18
19
20
21 **Word Count: 2695**

25 **Abstract (243 words)**

26 **Purpose:** The positional analysis of hepatic glycogen enrichment from deuterated water ($^2\text{H}_2\text{O}$)
27 by ^2H NMR has been previously applied to resolve the contributions of glucose and fructose to
28 glycogen synthesis in rodents fed a high sucrose diet. To further validate this method, this analysis
29 was applied to mice fed with synthetic diets whose carbohydrate components were comprised solely
30 of either glucose or fructose.

31 **Methods:** Eight glucose- and twelve fructose-fed mice (GLU-mice and FRU-mice) were given
32 $^2\text{H}_2\text{O}$ followed by *ad-libitum* feeding overnight. Mice were then euthanized, hepatic glycogen was
33 isolated and derivatized to monoacetone glucose, and ^2H -enrichment of positions 2, 5 and 6_s was
34 measured by ^2H NMR. From these data, the fraction of overnight glycogen appearance from the
35 direct pathway and/or glycogen cycling and indirect pathway were estimated. Indirect pathway
36 fractions were resolved into Krebs cycle and triose-P sources – the latter including contributions
37 from fructose metabolism.

38 **Results:** After overnight feeding, the fraction of overnight glycogen appearance derived from
39 direct pathway and/or glycogen cycling in GLU-mice was $63\pm 1\%$. For the indirect pathway, Krebs
40 cycle and triose-P sources contributed $22\pm 1\%$ and $15\pm 1\%$, respectively. For FRU-mice, glycogen
41 appearance was dominated by triose-P sources ($60\pm 2\%$) with lesser contributions from Krebs cycle
42 ($14\pm 2\%$) and direct and/or glycogen cycling ($26\pm 2\%$).

43 **Conclusions:** ^2H NMR analysis of hepatic glycogen ^2H -enrichment from $^2\text{H}_2\text{O}$ provides realistic
44 profiles of dietary glucose and fructose contributions to hepatic glycogen synthesis in mice fed with
45 diets containing one or the other sugar as the sole carbohydrate source.

46

47 **Keywords:** gluconeogenesis, deuterated water, indirect pathway, ^2H NMR.

48

49 **Introduction:** In Westernized societies, the surge in obesity and related complications such
50 as Type 2 diabetes and non-alcoholic fatty liver disease has in part been attributed to increased
51 consumption of refined sugar in the form of sucrose or high-fructose corn syrup. Since the liver is
52 among the first sites in the body to intercept glucose and fructose from these sources, there is
53 substantial interest in hepatic metabolism of these sugars. In contrast to glucose, hepatic conversion
54 of fructose to triose phosphates (triose-P) is not regulated by insulin. When dietary fructose is
55 abundant, the resulting high inflow of triose-P promotes hepatic glycogen synthesis via the indirect
56 pathway (Figure 1). We previously demonstrated in rat models that glycogen synthesis via direct
57 and indirect pathways can be quantified during natural overnight using deuterated water ($^2\text{H}_2\text{O}$) (1).
58 Subsequently, we demonstrated that indirect pathway contributions can be additionally resolved
59 into substrates that enter at the level of triose-P - which include fructose - and those that are
60 metabolized via Krebs cycle anaplerosis (2). This analysis revealed a significant increase in
61 indirect pathway triose-P contributions to glycogen synthesis in rats whose normal chow diet was
62 supplemented with sucrose in the drinking water. This increase in triose-P contribution was
63 explained by glycogenic metabolism of the fructose component of sucrose. Since dietary glucose
64 sources were more plentiful than that of fructose in these studies¹, we hypothesized that if fructose
65 was the dominant dietary sugar, then hepatic glycogen synthesis should be skewed even further
66 towards indirect pathway triose-P sources and this would be reflected in the ^2H -enrichment
67 distribution of glycogen. Conversely, if fructose was completely absent and dietary carbohydrate
68 was comprised entirely of glucose, then hepatic glycogen synthesis from triose-P sources should be
69 minimal, while direct pathway contributions would dominate. We tested this hypothesis by
70 measuring the sources of hepatic glycogen synthesis in two groups of mice: one group fed a
71 synthetic diet where fructose was the sole carbohydrate component and the other fed a diet with
72 glucose as the sole carbohydrate.

73

¹ Glucose equivalents from the drinking water sucrose plus additional glucose derived from maltose in the chow.

74 **Methods**

75 *Materials:* $^2\text{H}_2\text{O}$ at 99.9% enrichment was obtained from Eurisotop, Saint-Aubain, France.

76

77 *Animal Studies:* Animal studies were approved by the University of Coimbra Ethics Committee on
78 Animal Studies (ORBEA) and the Portuguese National Authority for Animal Health (DGAV),
79 approval code 0421/000/000/2013. Adult male C57BL/6 mice were obtained from Charles River
80 Labs, Barcelona, Spain, and housed at the University of Coimbra Faculty of Medicine Bioterium.
81 They were maintained with a 12h light/12h dark cycle. Upon delivery to the Bioterium, mice were
82 provided a two week interval for acclimation, with free access to water and standard chow,
83 comprising of 60% mixed carbohydrate, 16% protein and 3% lipid. After this period, animals were
84 randomly assigned to two synthetic diets formulated on an AIN-93G background and supplied by
85 Special Diets Services, Argenteuil, France for a 10-week period. The first formulation consisted of
86 60% glucose, 16% protein and 3% lipid by weight and the second consisted of 60% fructose, 16%
87 protein and 3% lipid by weight. These synthetic diets were packaged in coarse powder form. For
88 this reason, the mice were provided with the powdered standard chow placed in small open Petri
89 dishes during the initial 2-week adjustment period and this method of feed delivery was used in the
90 subsequent studies. Fasting glucose levels and glucose tolerance were assessed at baseline and at
91 the start of weeks 5 and 10 of the feeding trial. Mice were fasted throughout the dark period and
92 through the initial 4 h of the light period for a total time of 16 h. They were gavaged with a solution
93 of 10% glucose prepared in sterilized drinking water whose volume corresponded to 2 mg glucose/g
94 body weight. Blood glucose levels were monitored from tail tip samples at 0, 15, 30, 60 and 120
95 min after gavage using a OneTouch Vita (LifeScan) glucometer and glucose tolerance was assessed
96 by the area under the curve over 0-120 min.

97 On the ultimate evening of the feeding trial, mice were given an intraperitoneal injection of 99.9%
98 $^2\text{H}_2\text{O}$ with 0.9% w/v NaCl at a dose of 3 grams/100 g body weight at the start of the dark cycle. At
99 the same time, the drinking water was supplemented with 99.9% $^2\text{H}_2\text{O}$ (5% v/v). At the end of this

100 dark cycle, mice were anesthetized with halothane and sacrificed by cervical dislocation. Arterial
101 blood was collected and rapidly centrifuged for plasma collection and livers were freeze-clamped.
102 Plasma and livers were stored at -80 °C until further analysis. In a separate study, 12 adult mice fed
103 with standard chow were maintained under the same conditions. Their drinking water was
104 supplemented at the start of the dark period with 15% w/w glucose enriched to 20% with [U-
105 ²H₇]glucose, and 15% w/v unlabelled fructose. After *ad libitum* feeding and drinking overnight, the
106 mice were euthanized, and liver glycogen was extracted and analysed by ²H NMR as described
107 below. The ratio of glycogen enrichment in positions 2 and 3 was used to calculate the correction
108 factor for incomplete glucose-6-phosphate-fructose-6-phosphate exchange as previously described
109 (6).

110

111 *Glycogen extraction and monoacetone glucose synthesis:* Samples were prepared as described
112 previously by Rito et al. (3) Briefly, glycogen was extracted from frozen liver powder by treatment
113 with 30% KOH (2 ml/g of liver) at 70°C for 30 minutes. The mixture was treated with 6% Na₂SO₄
114 (1 ml/g of liver) and glycogen precipitated with ethanol (7 ml/g of liver). After centrifugation, the
115 solid residue was dried and resuspended in acetate buffer (0.05 M, pH = 4.5). Aqueous solution
116 containing 16 U of amyloglucosidase from *Aspergillus niger* (Glucose-free preparation, Sigma-
117 Aldrich, Germany) was added and incubated overnight at 55°C. The supernatant was lyophilized
118 and mixed with 5 ml ²H-enriched acetone prepared as described (4) and 4% sulphuric acid enriched
119 to 2% with ²H₂SO₄ (v/v). The mixture was stirred overnight at room temperature. The reaction was
120 quenched with water (5 ml, enriched to 2% with ²H₂O), the pH adjusted with HCl (pH 2.0) and the
121 mixture incubated at 40°C for 5 hours. The solution pH was adjusted to 8 with NaHCO₃ and the
122 samples evaporated to dryness. Monoacetone glucose (MAG) in the residue was extracted with
123 boiling ethyl acetate. Ethyl acetate was evaporated, the residue dissolved in H₂O and purified by
124 solid phase Discovery[®] DSC-18 3 mL/500 mg disposable columns (Sigma-Aldrich) as previously
125 described (3).

126

127 *NMR analysis:* Proton-decoupled ^2H NMR spectra were obtained with a Varian VNMRS 600
128 MHz NMR (Agilent) spectrometer equipped with a 3-mm broadband probe. Plasma body water ^2H -
129 enrichments were determined from 10 μL of plasma by ^2H NMR as described previously (5). MAG
130 samples were dissolved in 90% acetonitrile/10% water and the ^2H NMR spectra were acquired at 50
131 $^{\circ}\text{C}$ using a 90° pulse and 1.7 s of recycling time (1.6 s of acquisition time and 0.1 s pulse delay). The
132 spectra were processed with 1.0 Hz line-broadening before Fourier transformation. Positional ^2H
133 enrichments were determined from the known enrichment of MAG methyl signals that were used as
134 an internal standard. Spectra were analyzed using NUTS PC-based NMR spectral analysis software
135 (Acorn NMR Inc., USA).

136

137 *Quantification of the sources of hepatic glycogen appearance:* The fractional contributions of
138 direct pathway, indirect pathway sources via Krebs cycle and indirect pathway sources via triose-P
139 to overnight glycogen appearance were quantified from glycogen positions 2, 5 and 6s (H2, H5 and
140 H6s) using the following three equations (2).

141

142 Equation 1: Direct pathway and/or glycogen cycling = $100 \times (1 - \text{H5}/\text{H2})$

143 Equation 2: Indirect pathway sources via Krebs cycle = $100 \times \text{H6s}/\text{H2}$

144 Equation 3: Indirect pathway sources via Triose-P = $100 \times (\text{H5} - \text{H6s})/\text{H2}$

145

146 H2 was adjusted for the known incomplete exchange of body water and position 2 hydrogens via
147 glucose-6-phosphate isomerase (6). Since glycogen cycling (glycogen \rightarrow Glu-1-P \leftrightarrow Glu-6-P \leftrightarrow
148 Fru-6-P \leftrightarrow Glu-6-P \leftrightarrow Glu-1-P \rightarrow UDPG \rightarrow glycogen) can result in the selective enrichment of
149 position 2 (7) thereby mimicking direct pathway contributions, we reported this activity as direct
150 pathway and/or glycogen cycling.

151

152 *Statistics:* All results are presented as means \pm standard error and comparisons were made by
153 an unpaired t-test (two tailed) performed using Microsoft Excel.
154

155 **Results**

156 The two groups of mice showed equal weight gains over the 10 week feeding trial (24.0 ± 0.4 g to
157 26.2 ± 0.6 g for GLU-mice and 22.6 ± 0.6 g to 24.6 ± 0.4 g for FRU-mice. The two groups also had
158 equal fasting glucose levels and glucose tolerance at baseline as well as in the fifth and tenth week
159 of feeding (data not shown). Body water enrichments had a tendency to be higher in fructose-fed
160 (FRU-mice) compared to glucose-fed mice (GLU-mice), as shown in Table 1, but the difference
161 was not significant ($p = 0.18$). Figure 2 shows representative ^2H NMR spectra of derivatized
162 glycogen obtained from a FRU-mouse **a**), and a GLU-mouse **b**). The spectra had well-resolved
163 signals with high signal-to-noise ratios from all seven hydrogens attached to the hexose carbon
164 skeleton allowing precise quantification of positional ^2H -enrichment in all sites (Table 1). The
165 glycogen spectrum from the FRU-mouse showed low enrichment of position 6_S (as well as 6_R)
166 relative to position 5 indicating a high abundance of glycogen enriched in position 5 but not in
167 position 6_S over that enriched in both positions. As indicated by Figure 1, this implies a high
168 contribution of substrates entering glycogenesis at the level of Triose-P such as fructose, over
169 substrates that originated via Krebs cycle anaplerosis. Another noteworthy feature of spectra from
170 FRU-mice was that the enrichment of position 2 was significantly lower than that of position 5 ($p =$
171 0.003). Assuming complete exchange between water and metabolite hydrogens at the various steps
172 of the glycolytic pathways shown in Figure 1, enrichment of position 2 can never be exceeded by
173 that of position 5. We developed an assay for quantifying the fraction of G6P hydrogen 2
174 exchanged during direct pathway glycogenesis based on the retention of ^2H in glycogen position 2
175 relative to position 3 following $[\text{U-}^2\text{H}_7]\text{glucose}$ metabolism (6). Our previous studies in fish (3,8)
176 and in rats (6) indicate that under conditions of hepatic glycogen synthesis, exchange of body water
177 and position 2 hydrogens via glucose-6-phosphate isomerase (G6PI) is substantially incomplete
178 regardless of direct or indirect pathway contributions. This, rather than any analytical artefact,
179 provides a satisfactory explanation for the lower than expected position 2 enrichment. We therefore
180 applied the $[\text{U-}^2\text{H}_7]\text{glucose}$ assay to mice and obtained a correction factor (1.57 ± 0.03) that

181 allowed position 2 enrichment to be adjusted for incomplete G6PI-mediated exchange (6). This
182 value is similar to that reported previously in rats (1.64) (6). The adjusted position 2 enrichments
183 are shown alongside the measured ones in Table 1.

184 Based on the adjusted enrichment of position 2 and the unadjusted enrichments of positions
185 5, and 6_S, the fractional contributions of direct pathway and/or cycling, indirect pathway from
186 substrates entering at the level of triose-P, and indirect pathway contributions via the Krebs cycle to
187 overnight glycogen appearance were calculated and are shown in Table 1. In FRU-mice, the
188 majority of overnight glycogen appearance was derived from substrates directly feeding triose-P –
189 consistent with glycogenesis from fructose. Direct pathway and/or cycling and Krebs cycle sources
190 accounted for only minor portions. The glycogen synthesis profile of GLU-mice was markedly
191 different, with direct pathway + glycogen cycling activities accounting for the bulk of newly-
192 appeared glycogen. Moreover, indirect pathway contributions from the Krebs cycle exceeded those
193 from triose-P substrates.

194

195 **Discussion**

196 Since the concept of hepatic glycogen synthesis via gluconeogenic intermediates, referred to as the
197 indirect pathway, was advanced and validated experimentally (9,10) the activity and role of this
198 pathway has been studied under various physiological and pathophysiological conditions (11-14).
199 However to date, relatively little attention has been paid to the sources of indirect pathway carbons
200 despite the early realization that any gluconeogenic substrate could in principle feed the indirect
201 pathway (10). Since fructose is initially metabolized to triose-P, the indirect pathway is obligatory
202 for its conversion to glycogen. There is extensive evidence that fructose *per se* is a potent
203 glycogenic substrate. Substrate balance studies in fasted dogs have shown that intraportally-infused
204 fructose results in the rapid synthesis of hepatic glycogen to supraphysiological levels (15,16).
205 Intravenous infusion of fructose into healthy humans subjects resulted in an increased flux through
206 UDP-glucose, indicative of increased glycogen synthase activity (17). Our observations of triose-P

207 sources being the dominant source of hepatic glycogen synthesis in the FRU-mice are fully
208 consistent with these previous studies. For mice given glucose as the sole dietary carbohydrate,
209 direct pathway and/or glycogen cycling was the dominant contributor to overnight glycogen
210 appearance. If hepatic glycogen turnover is incomplete², the ²H₂O method *per se* cannot resolve
211 direct pathway and glycogen cycling fluxes. This requires an independent measurement of net
212 hepatic glycogen synthesis (7,18) or the integration of ²H₂O and [U-¹³C]glucose tracers (3).

213 FRU-mice had a sizable contribution of glycogen enriched in position 2 only, indicative of
214 direct pathway metabolism of unlabeled glucose or glycogen cycling activity. Since dietary sources
215 of glucose were absent from the feed of FRU-mice, we conclude that glycogen cycling was solely
216 responsible for this activity. In healthy human subjects, glycogen cycling was shown to be
217 increased during infusion of substrate levels of fructose (19).

218 Our analysis makes several assumptions on substrate availability and metabolism. As
219 indicated in Figure 1, the ²H-enrichment profile of glycogen synthesized from fructose is identical
220 to that formed from glycerol, hence contributions from these two substrates cannot be distinguished.
221 Given that under fed conditions, circulating glycerol levels are low and that glycerol-3-phosphate
222 flux is directed towards fatty acid esterification rather than gluconeogenesis, its contribution to
223 glycogen synthesis is likely to be minimal. Concerning the metabolism of fructose, if its triose-P
224 products initially feed into pyruvate and anaplerotic pathways instead of being directly converted to
225 hexose-P, then these will be indistinguishable from other anaplerotic indirect pathway precursors.
226 The low overall contribution of Krebs cycle sources to glycogen turnover in FRU-mice suggests
227 that fructose metabolism by this route was relatively minor. Our unpublished observations of
228 glycogen enrichment from [U-¹³C]fructose also indicate relatively low levels of label randomization
229 via the Krebs cycle. In our initial studies of glycogen enrichment from ²H₂O, exchange of G6P
230 position 2 and body water was assumed to be complete (1,2). However, later studies showed
231 substantially incomplete exchange in both fish and rats (6) while a human study indicated near-

² Pre-existing unlabeled glycogen is converted to [2-²H]glycogen via glycogen cycling. When glycogen turnover is complete, new [2-²H]glycogen can only be generated by the direct pathway metabolism of dietary glucose.

232 complete exchange (20). In this report, we confirmed that G6P position 2 and body water exchange
233 was also incomplete for mice fed normal chow and drinking water supplemented with glucose and
234 fructose hence a correction factor was applied to the measured position 2 enrichment. To the extent
235 that this correction factor differs between this setting and those of the synthetic glucose and fructose
236 diets, the corrected position 2 enrichment and fractional flux estimates will have systematic errors.

237 In conclusion, we demonstrated that the ^2H -enrichment distribution of hepatic glycogen
238 from $^2\text{H}_2\text{O}$ in mice informs the contributions of dietary glucose and fructose to hepatic glycogen
239 synthesis via direct and indirect pathways under natural feeding conditions. This approach may be
240 useful for furthering our understanding of the relationship between hepatic glycogen metabolism
241 and dietary carbohydrate composition.

242

243 **Acknowledgements:** The authors acknowledge financial support from the Portuguese Foundation
244 for Science and Technology (research grants PTDC/SAU~MET/11138/2009 and
245 EXCL/DTP/0069/2012). Structural funding for the Center for Neurosciences and the UC-NMR
246 facility is supported in part by FEDER – European Regional Development Fund through the
247 COMPETE Programme and the Portuguese Foundation for Science and Technology through grants
248 PEst-C/SAU/LA0001/2011; REEQ/481/QUI/2006, RECI/QEQ-QFI/0168/2012, CENTRO-07-
249 CT62-FEDER-002012, and Rede Nacional de Ressonância Magnética Nuclear. The fellowship of
250 GDW is supported by the European Union’s Horizon 2020 Research and Innovation programme
251 under the Marie Skłodowska-Curie Grant Agreement No. 722619.

252

253 **Footnotes:** 1. Glucose equivalents from the drinking water sucrose plus additional glucose
254 derived from maltose in the chow.
255 2. Pre-existing unlabeled glycogen is converted to $[2\text{-}^2\text{H}]$ glycogen via glycogen
256 cycling. When glycogen turnover is complete, new $[2\text{-}^2\text{H}]$ glycogen can only be
257 generated by the direct pathway metabolism of dietary glucose.

References

1. Soares AF, Viegas I, Carvalho RA, Jones JG. Quantifying hepatic glycogen synthesis by direct and indirect pathways in rats under normal *ad libitum* feeding conditions. *Magnetic Resonance in Medicine* 2009;61:1-5.
2. Delgado TC, Martins FO, Carvalho F, Goncalves A, Scott DK, O'Doherty R, Macedo MP, Jones JG. ^2H enrichment distribution of hepatic glycogen from $^2\text{H}_2\text{O}$ reveals the contribution of dietary fructose to glycogen synthesis. *American Journal of Physiology - Endocrinology and Metabolism* 2013;304:E384-391.
3. Rito J, Viegas I, Pardal MA, Meton I, Baanante IV, Jones JG. Disposition of a glucose load into hepatic glycogen by direct and indirect pathways in juvenile seabass and seabream. *Scientific Reports* 2018;8.
4. Jones JG, Barosa C, Gomes F, Mendes AC, Delgado TC, Diogo L, Garcia P, Bastos M, Barros L, Fagulha A, Baptista C, Carvalheiro M, Caldeira MM. NMR derivatives for quantification of ^2H and ^{13}C -enrichment of human glucuronide from metabolic tracers. *Journal of Carbohydrate Chemistry* 2006;25:203-217.
5. Jones JG, Merritt M, Malloy C. Quantifying tracer levels of $^2\text{H}_2\text{O}$ enrichment from microliter amounts of plasma and urine by ^2H NMR. *Magn Res Med* 2001;45:156-158.
6. Martins FO, Rito J, Jarak I, Viegas I, Pardal MA, Macedo MP, Jones JG. Disposition of U- $^2\text{H}_7$]glucose into hepatic glycogen in rat and in seabass. *Comparative Biochemistry and Physiology A, Molecular & integrative physiology* 2013;166:316-322.
7. Kacerovsky M, Jones J, Schmid AI, Barosa C, Lettner A, Kacerovsky-Bielez G, Szendroedi J, Chmelik M, Nowotny P, Chandramouli V, Wolzt M, Roden M. Postprandial and Fasting Hepatic Glucose Fluxes in Long-Standing Type 1 Diabetes. *Diabetes* 2011;60:1752-1758.
8. Viegas I, Rito J, Jarak I, Leston S, Carvalho RA, Meton I, Pardal MA, Baanante IV, Jones JG. Hepatic glycogen synthesis in farmed European seabass (*Dicentrarchus labrax* L.) is

dominated by indirect pathway fluxes. *Comparative Biochemistry and Physiology A-Molecular & Integrative Physiology* 2012;163:22-29.

9. Newgard CB, Hirsch LJ, Foster DW, McGarry JD. Studies on the mechanism by which exogenous glucose is converted into liver-glycogen in the rat - a direct or an indirect pathway. *Journal of Biological Chemistry* 1983;258:8046-8052.
10. Newgard CB, Moore SV, Foster DW, McGarry JD. Efficient hepatic glycogen-synthesis in refeeding rats requires continued carbon flow through the gluconeogenic pathway. *Journal of Biological Chemistry* 1984;259:6958-6963.
11. Bischof MG, Bernroider E, Krssak M, Krebs M, Stingl H, Nowotny P, Yu C, Shulman GI, Waldhausl W, Roden M. Hepatic glycogen metabolism in type 1 diabetes after long-term near normoglycemia. *Diabetes* 2002;51:49-54.
12. Nielsen MF, Wise S, Dinneen SF, Schwenk WF, Basu A, Rizza RA. Assessment of hepatic sensitivity to glucagon in NIDDM - Use as a tool to estimate the contribution of the indirect pathway to nocturnal glycogen synthesis. *Diabetes* 1997;46:2007-2016.
13. Petersen KF, Laurent D, Yu CL, Cline GW, Shulman GI. Stimulating effects of low-dose fructose on insulin-stimulated hepatic glycogen synthesis in humans. *Diabetes* 2001;50:1263-1268.
14. Jones JG, Fagulha A, Barosa C, Bastos M, Barros L, Baptista C, Caldeira MM, Carvalheiro M. Noninvasive analysis of hepatic glycogen kinetics before and after breakfast with deuterated water and acetaminophen. *Diabetes* 2006;55:2294-2300.
15. Winnick JJ, Kraft G, Gregory JM, Edgerton DS, Williams P, Hajizadeh IA, Kamal MZ, Smith M, Farmer B, Scott M, Neal D, Donahue EP, Allen E, Cherrington AD. Hepatic glycogen can regulate hypoglycemic counterregulation via a liver-brain axis. *Journal of Clinical Investigation* 2016;126:2236-2248.

16. Pagliassotti MJ, Holste LC, Moore MC, Neal DW, Cherrington AD. Comparison of the time courses of insulin and the portal signal on hepatic glucose and glycogen metabolism in the conscious dog. *Journal of Clinical Investigation* 1996;97:81-91.
17. Dirlewanger M, Schneiter P, Jequier E, Tappy L. Effects of fructose on hepatic glucose metabolism in humans. *American Journal of Physiology-Endocrinology and Metabolism* 2000;279:E907-E911.
18. Stingl H, Chandramouli V, Schumann WC, Brehm A, Nowotny P, Waldhäusl W, Landau BR, Roden M. Changes in hepatic glycogen cycling during a glucose load in healthy humans. *Diabetologia* 2006;49:360-368.
19. Tounian P, Schneiter P, Henry S, Jequier E, Tappy L. Effects of infused fructose on endogenous glucose-production, gluconeogenesis, and glycogen-metabolism. *American Journal of Physiology-Endocrinology and Metabolism* 1994;267:E710-E717.
20. Barosa C, Silva C, Fagulha A, Barros L, Caldeira MM, Carvalheiro M and Jones JG. Sources of hepatic glycogen synthesis following a milk-containing breakfast meal in healthy subjects. *Metabolism: Clinical and Experimental* 2012;61:250-254.

Figure Legends

Figure 1: Schematic of glycogen synthesis from fructose and glucose and positional enrichment of glycogen from $^2\text{H}_2\text{O}$. For clarity, some metabolic intermediates have been omitted. Glycogen derived via direct pathway metabolism of glucose (Glucose \rightarrow Glu-6-P \rightarrow Glu-1-P \rightarrow UDPG \rightarrow Glycogen) or undergoing cycling following hydrolysis to Glu-1-P (blue arrow) will be enriched in position 2 (**A**). Glycogen derived from triose-P sources, including fructose, will be enriched in positions 2 and 5 (**B**). Glycogen derived from pyruvate (which may originate from glucose metabolized peripherally via the Cori cycle or from hepatic glycolysis) or from any other anaplerotic Krebs cycle substrate (not shown) will be enriched in positions 2, 5 and 6s (**C**).

Figure 2: ^2H NMR spectra of monoacetone glucose derived from liver glycogen of a mouse fed with a diet where fructose was the sole carbohydrate **a**) and a diet where glucose was the sole carbohydrate **b**). The numbers above the signals indicate their glucosyl positional origin.

Table 1: Glycogen and body water ²H-enrichments and fractional contributions of various sources to overnight glycogen appearance following ²H₂O administration for mice fed with diets whose carbohydrate component consisted either entirely of fructose or of glucose. Data are shown as means with standard errors in parentheses below each value. *Position 2 enrichment after correction for incomplete exchange of ²H between water and glucose-6-P position 2.

Diet	Glycogen positional enrichments and body water (BW) enrichment									Glycogen appearance sources (%)		
	1	2	2*	3	4	5	6R	6S	BW	Direct and/or cycling	Indirect-Triose-P	Indirect-Krebs cycle
Fructose (n=12)	0.67 (0.09)	1.43 (0.04)	2.26 (0.07)	1.32 (0.04)	1.52 (0.04)	1.66 (0.05)	0.35 (0.02)	0.32 (0.01)	2.70 (0.01)	26 ^a (2)	60 ^b (2)	14 ^c (1)
Glucose (n=8)	0.59 (0.09)	1.01 (0.14)	1.60 (0.23)	0.46 (0.07)	0.58 (0.08)	0.59 (0.09)	0.36 (0.06)	0.38 (0.07)	2.26 (0.07)	63 (1)	15 (1)	22 (1)

^a $p = 3 \times 10^{-10}$ compared to glucose; ^b $p = 1 \times 10^{-12}$ compared to glucose; ^c $p = 2 \times 10^{-4}$ compared to glucose.

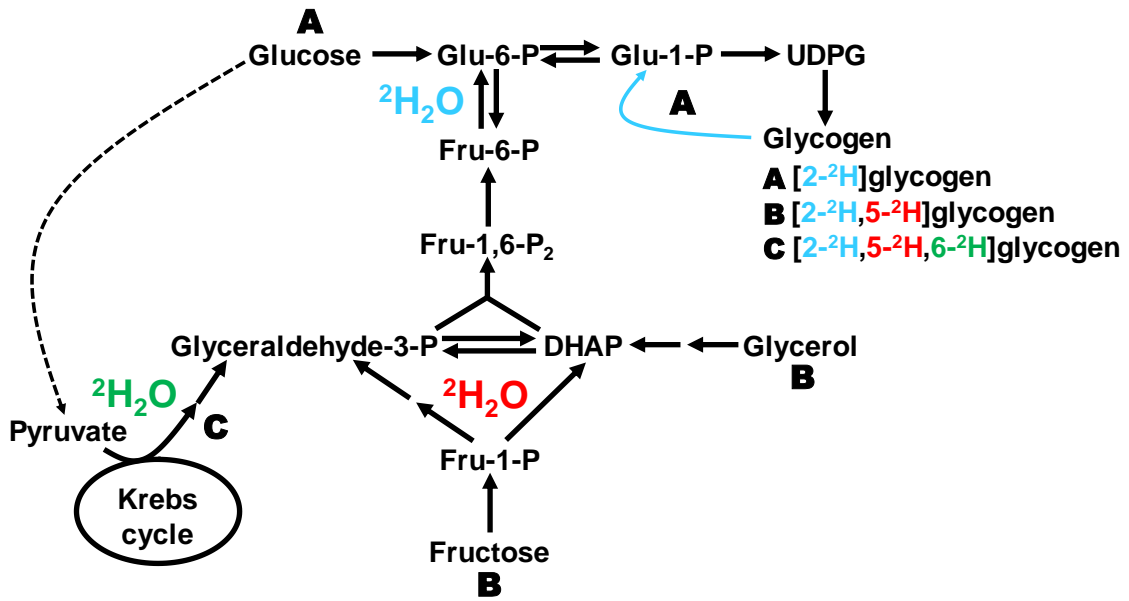


Figure 1

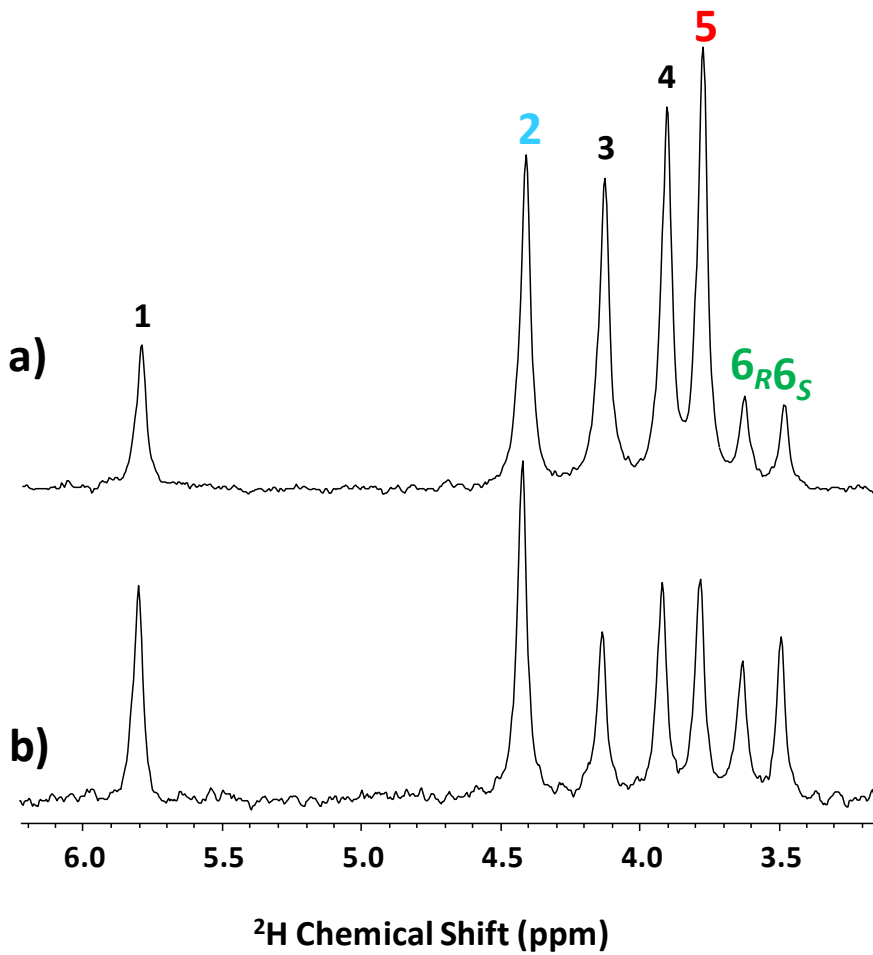


Figure 2